Fast Radiation Parameterization Schemes for Mesoscale and Short-Range Forecast Models

HANNU SAVIJÄRVI

Department of Meteorology, University of Helsinki, Helsinki, Finland

(Manuscript received 11 February 1989, in final form 27 June 1989)

ABSTRACT

Three fast and simple longwave broadband radiation parameterization schemes were tested against a reference narrow-band model in clear sky conditions. The three schemes gave rather similar results. The emissivity dependence on water vapor path length was tuned to give best fit to the reference. The smaller other gas, aerosol and continuum effects were added in a simple fashion both to the radiative cooling and to the longwave downward flux at the surface. Clouds are handled as blackbodies.

In the shortwave scheme the attenuation of solar radiation due to variable water vapor and gray clouds, but average ozone and other gas absorption, aerosols and Rayleigh scattering are taken into account and tuned by surface observations of solar flux. The water vapor absorptivity for solar heating was fitted by line-by-line model results.

1. Introduction

With the advance of numerical modeling the parameterization of radiation is beginning to be included in many mesoscale and high-resolution short-range forecast models. However, the radiative longwave cooling of the atmosphere and daytime heating due to absorption of solar shortwave radiation tend to be only small terms in these model applications. Therefore, the rather accurate but very time-consuming line-by-line integrations of the radiative transfer equations are not appropriate. Even broadband or emissivity methods may be too time consuming to be cost effective for short-range forecasting or some mesoscale model applications. For this reason, very simple and fast methods of radiative parameterization are compared here with better schemes and observations of radiative fluxes and heating to validate them for error-insensitive applications.

The first longwave method was suggested by Rogers and Walshaw (1966) (RW) as the "cooling to space" approximation. The second method is attributed to Sasamori (1972). It was used for example by McNider and Pielke (1981) and has become popular after recommendation in Pielke's (1984) book. Third, the traditional emissivity method is the direct vertical integration of the radiative transfer equations to get the upward and downward fluxes and then the cooling rate as the vertical divergence of the net flux. This method is described in textbooks (e.g., Houghton 1984) and is, in principle, more accurate, but also more time-consuming, than the two others, which are approximations of it. Fels and Schwartzkopf (1975) and Wu (1980) criticize these methods in GCM use, but they might still be adequate in the less demanding applications.

In this report, these three approximations are compared against the narrowband calculation of RW for clear sky conditions. Some sensitivity tests are made. It is acknowledged that the RW method may not be the best reference around, however, its results are readily available and have been widely used for comparisons (e.g., Garand 1984). The accuracy of the RW cooling rate is perhaps only a few tenths of K day^{-1} (Morcrette and Fouquart 1985). When observations or line-by-line model results become openly available in the literature, the present methods can be retuned to them. Unfortunately, the observations of longwave radiative fluxes are not very accurate or abundant. A comparison is made here to a set of Suomi–Kuhn radiometer tropical soundings reported in Cox (1969).

Based on the comparisons, an improved emissivity curve for the water vapor line spectrum is suggested. The water vapor continuum problem is discussed and a very crude but fast approximation for it and the CO_2, other gases, and aerosol effects is described. Finally, a fast shortwave broadband parameterization is also presented (based partly on published line-by-line model results, Chou 1986) and compared to surface and free atmosphere solar radiation observations. Clouds are treated here simply as gray- or blackbodies; better cloud schemes and impact studies are underway.

The targeted tolerance, i.e. difference to the references (RW and observations), is set to 0.3 K day^{-1} in

Corresponding author address: Dr. Hannu Savijärvi, Department of Meteorology, University of Helsinki, Helsinki, Finland.

the cooling rates and 10 W m^{-2} in the fluxes, and interest is given only to the troposphere. The methods chosen should be as fast as possible within these limits. The computer time thus saved can then be used for the more important forcing mechanisms or increased resolution in the host model. Fast radiation methods might be useful also in e.g., agrometeorology and surface heat budget studies.

The aim of this paper lies in short-range forecasting. Thus the methods are kept crude but are extremely fast. They cannot justify themselves e.g., in GCMs, where even tiny systematic errors may be serious in the long run, nor in detailed PBL models, especially if clouds are present.

2. Longwave broadband radiation schemes

Because computation speed is the decisive factor here, we concentrate only in the emissivity (i.e. broadband) methods, where the integration over the frequency domain is done once and for all. The error caused by the frequency integration will be minimized by selecting the emissivity curve optimally.

The clear sky downward longwave radiative flux is, following Stephens (1984):

$$F^{\downarrow}(z) = \int_0^{\infty} \int_z^{\infty} \frac{dA_\nu}{dz'}(z, z')\pi B_\nu(z')dz'd\nu, \quad (1)$$

where A_ν is the absorptivity of the gas(es), ν frequency, and B_ν the Planck function. If the emissivity ϵ along the vertical path $z \rightarrow z'$ is defined as the mean absorption weighted by the Planck function,

$$\epsilon(z, z') = \frac{1}{\sigma T^4} \int_0^{\infty} A_\nu(z, z')\pi B_\nu(T)d\nu, \quad (2)$$

the downward flux becomes

$$F^{\downarrow}(z) = \int_z^{\infty} \frac{d\epsilon}{dz}(z, z')\sigma T^4(z')dz'. \quad (3)$$

For a path with constant p and T between z and z', (2) is the definition of homogeneous emissivity. It can be calculated from the spectral properties of the gas(es) or measured in the laboratory. The accuracy in both methods is far from perfect, and, moreover, the path is always nonhomogeneous in the real atmosphere. Therefore, the emissivity curve is perhaps best defined by fitting the results to some reference values (c.f. Rogers 1967). This will be done in section 3a.

For upward flux calculations the form similar to (3) is rather inaccurate in finite vertical resolution computations, as noted by Rogers (1977) (and verified by numerical testing). Therefore, it is better to define a new emissivity through

$$\epsilon'(z, z') = \int_0^{\infty} A_\nu(z, z') \frac{dB_\nu}{d\sigma T^4(z')} d\nu. \quad (4)$$

With this, and by using partial integration the upward flux becomes

$$F^{\uparrow}(z) = \sigma T_g^4 + \int_0^z \epsilon'(z, z') \frac{d\sigma T^4(z')}{dz'} dz'. \quad (5)$$

Since the shape of dB_ν/dT is similar to that of B_ν, ϵ' is nearly the same as ϵ except for a constant. This was demonstrated in Fig. 6 of Stephens (1984) where ϵ' and ϵ from several sources were compared as the function of water vapor pathlength. Based on this figure and numerical testing, ϵ' is fixed to $\epsilon - 0.05$ in what follows.

Once the upward and downward fluxes are calculated, the temperature change is given by the vertical divergence of the net flux:

$$\left(\frac{\partial T}{\partial t}\right)_{\text{LWR}} = -\frac{1}{\rho c_p}\frac{\partial}{\partial z}(F^{\uparrow} - F^{\downarrow}) = \frac{g}{c_p}\frac{\partial}{\partial p}F_{\text{net}}. \quad (6)$$

a. The integration method

The integration method is based on the direct use of (3), (5), and (6) by numerical integration and differentiation through data points (using centered differences and trapezoidal rule in the following). We will only concentrate on the water vapor line spectrum here and deal with the other gases, aerosols and the water vapor continuum later. For the water vapor line spectrum, a common approximate correction for the pressure and temperature dependence of the absorption/emission is made (the pressure scaling correction), by using an effective water vapor amount u: the actual vertical water vapor path length is multiplied by $(p/p_o)^n(T_o/T)^{0.5}$, where $p_o = 1013$ mb and $T_o = 273$ K. Thus

$$u(z, z') = \int_{p(z')}^{p(z)} q\left(\frac{p}{p_o}\right)^n\left(\frac{T_o}{T}\right)^{0.5}\frac{dp}{g} \quad (7)$$

where q is specific humidity and g, gravity. Now $\epsilon(z, z') = \epsilon(u(z, z'))$. The scaling constant n is set to 0.85, after Houghton (1984). Stephens (1984) suggests a range of 0.5–0.9 for n. The sensitivity of the results to n will be studied later. The unit of u is g cm^{-2} so u is given in cm of (pressure scaled) precipitable water.

b. The Sasamori method

Sasamori (1972) suggested that in the longwave radiation calculations the atmosphere could be taken isothermal at each calculation level. Then the height integrals in (3) and (5) can be calculated analytically using Riemann–Stieltjes integration at the ground and at the top, the temperatures of which must be given. The result is (Pielke 1984):

$$\left(\frac{\partial T}{\partial t}\right)_s = -\frac{\sigma}{\rho c_p}\left\{\frac{\partial \epsilon(0, z)}{\partial z}(T^4(z) - T_g^4) - \frac{\partial \epsilon(z, \infty)}{\partial z}(T_t^4 - T^4(z))\right\} \quad (8)$$

where index t refers to the top of the radiative medium and g to the ground.

The basis for Sasamori's suggestion is that the fluxes far from the height of interest are small and therefore do not contribute much to the integrals. Pielke (1984) presents McNider's unpublished comparison of (8) with the integral method using Wangara day-33 data. In that comparison, Sasamori's method gave very realistic results.

c. *Cooling to space*

Rogers and Walshaw (1966) and Rogers (1977) suggested that when reorganizing the cooling rate (6) with the emissivity fluxes (3) and (5) to a form

$$\left(\frac{\partial T}{\partial t}\right) = -\frac{1}{\rho c_p}\left\{\sigma T^4(z)\frac{\partial \epsilon(z,\infty)}{\partial z} + \sigma(T^4(z) - T_g^4)\frac{\partial \epsilon(0,z)}{\partial z} + \int_0^\infty (\pi B(z) - \pi B(z'))\frac{\partial^2 \epsilon(z,z')}{\partial z \partial z'}\,dz'\right\} \quad (9)$$

it can be shown that the first term in (9)—emission from level z to space ("cooling to space")—is usually dominant by a large margin for water vapor line spectrum in the earth's atmosphere. The second term is exchange of radiation with the surface. The third term is the internal exchange of radiation with all other layers in the atmosphere. Rogers (1977) indicates that this last term gives a contribution only in the neighborhood of changes in the lapse rate of temperature, and is usually negligible, as is the second term. It may be noted in passing that the Sasamori approximation (8) (with T_t set to 0) consists of the two first terms in (9). The last term is excluded since there is no internal exchange of radiation in an isothermal atmosphere.

Actually, RWs suggestion was made in the context of a narrowband model, which gave very realistic results as a cooling-to-space approximation. The emissivity version is

$$\left(\frac{\partial T}{\partial t}\right)_{\text{cts}} = -\frac{\sigma T^4(z)}{\rho c_p}\frac{\partial \epsilon(z,\infty)}{\partial z} = \frac{g}{c_p}\frac{\partial \epsilon(z,\infty)}{\partial p}\sigma T^4(p), \quad (10)$$

i.e. only the dominant term in (9) is taken into account. This cooling-to-space (cts) scheme can be recognized as Sasamori's scheme with its first term omitted and T_t set to zero. The cts scheme is very fast since there is no vertical integration: one just calculates the vertical derivative of emissivity at the pathlength calculated from above to level z and multiplies $B(z)$ with that. As Rogers (1977) pointed out, "Newtonian cooling" methods of radiation can be considered as linearizations of the cts scheme along a suitable temperature profile. Good results for the cts approximation would therefore support Newtonian forcing for radiation, which is often used in simple climate models as an ad hoc assumption.

3. Results and suggestions for longwave radiation

a. *Emissivity for water vapor line spectrum*

We start the comparisons by taking the "London tropical profile"; i.e. temperature and moisture for March at 0–10°N (London 1952), which has been used for many comparisons. Its T, q, and $u(z,\infty)$, $u(0,z)$ profiles are shown in Table 1, in which pressure scaling, $n = 0.85$, has been used. In the comparisons, the analytic emissivity curve $\epsilon(u)$ of Sasamori (1968; Eqs. 14 and 15) are first adopted. This dependency is based on Yamamoto's (1952) spectral calculations for water vapor line spectrum. It was used for many years in the NCAR GCM (Washington and Williamson 1977) and is also the basis of the Yamamoto radiation chart.

In Fig. 1 the cooling rates from the Yamamoto and Elsasser radiation charts are shown for the London profile, based on Goody's (1964) evaluation. Also shown is the Rogers and Walshaw (1966) (RW) narrowband model result, which serves here as a reference. The cooling curves obtained by the integration method, Sasamori approach (with $T_t = 0$), and cooling-to-space scheme [all three based on Yamamoto $\epsilon(u)$] are quite close to each other in Fig. 1, except near the surface where the Sasamori method gives too small cooling rates. In midtroposphere they differ much less from each other than from the other curves. The integration method is just a numerical integration of the Yamamoto radiation chart equations; thus the difference between it and the Yamamoto curve in Fig. 1 indicates

TABLE 1. The temperature and specific humidity profiles for mean March 0–10°N, and the pressure and temperature-scaled water vapor, vertical path lengths (after London 1952).

z km	p mb	T C	q g kg^{-1}	$u(z,\infty)$ cm	$u(0,z)$ cm
0	1011	27.7	18.98	3.89	—
1	900	22.8	12.67	2.25	1.65
2	802	18.2	9.36	1.32	2.57
3	715	13.3	6.90	0.77	3.13
4	636	7.8	4.91	0.43	3.46
5	562	2.0	3.44	0.23	3.66
6	496	−3.5	2.32	0.12	3.78
7	438	−10.0	1.44	0.058	3.84
8	385	−16.6	0.92	0.028	3.87
9	336	−23.2	0.48	0.012	3.88
10	293	−30.0	0.34	0.005	3.89
11	253	−38.6	0.13	0.002	3.89
12	217	−47.2	0.07	0.0007	3.89
13	185	−55.7	0.03	0.0003	3.89
14	156	−62.3	0.02	0.0001	3.89
15	131	−69.0	0.01	0.0001	3.89

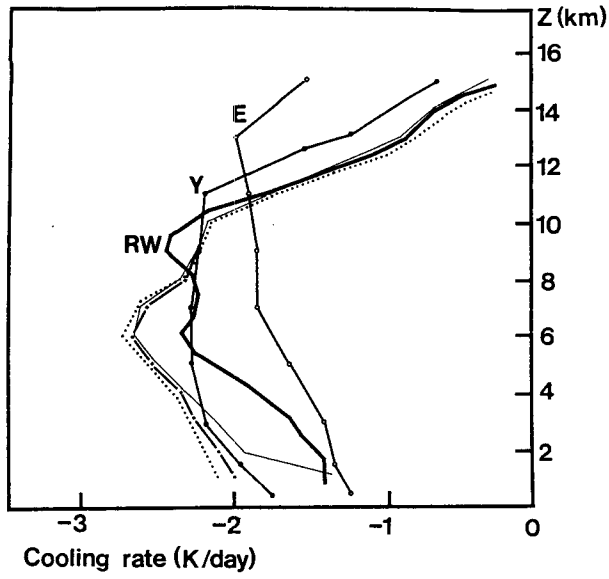

FIG. 1. The London profile cooling rates. RW = Rogers and Walshaw (1966), E = Elsasser chart, Y = Yamamoto chart. Dotted line = integral method, dash-dot line = cts method, thin line = Sasamori method. $\epsilon(u)$ from Sasamori (1968).

the level of inaccuracy that can be expected between the chart (graphical integration) and the numerical integration of the emissivity equations for the same $\epsilon(u)$.

Because the three tested methods are so close to each other, it is clear that even the simplest and fastest of them, the cts method, captures the essential cooling mechanism. The decisive factor in the cts method is $d\epsilon(u\ (z, \infty))/dz$ at any height. As can be seen from Table 1, $u(z, \infty)$ (which is the scaled precipitable water in cm above each level) decreases steadily upward. In contrast, $u(0, z)$ increases quickly upward near the surface, where most of the moisture lies. It remains nearly constant in the free atmosphere where $d\epsilon(u(0, z))/dz$ is thus small and the first term in the Sasamori method (8) becomes negligible. Consequently, the cts and Sasamori methods become nearly identical in the upper troposphere if $T_t = 0$.

It is now clear that $d\epsilon/dz$, or, equivalently, $d\epsilon/du$, should be chosen carefully. Unfortunately, $d\epsilon/du$ is not very well known. The values of $d\epsilon/dx$ (where $x = {}_{10}\log u$) of some emissivity formulations found in the literature are shown in Fig. 2. Of these, Yamamoto's (1952) and Elsasser's (1942) values are based on line-by-line or band-model calculations of water vapor line absorption. Staley and Jurica's (1970) values, recommended by Houghton (1984), are likewise theoretical but based on newer spectral data. Kuhn's (1963) emissivities are observational, based on fit of cooling from radiometer soundings to the integral method. Also Robinson's (1950) values are observational and form the basis of the Kew radiation chart.

In Fig. 1 it was seen that when compared to the RW scheme cooling from Elsasser's chart is too low at mid-tropospheric levels and too high in the stratosphere, while cooling from Yamamoto's $\epsilon(u)$ (both chart and numerical methods based on it) is too high in the lower troposphere but reasonably good in the upper troposphere and stratosphere where $u(z, \infty)$ (and thus, x) is small. Houghton (1984) notes the same general trend and suggests further that Elsasser's and Robinson's charts are at their best near the surface, where $u(z, \infty)$ and, x) is large. Therefore, it may be feasible to fit a curve to the values in Fig. 2 so that the curve is close to Yamamoto's $d\epsilon/dx$ at low values of x, but at high x, close to Elsasser's and Robinson's $d\epsilon/dx$. For medium x, the curve should be somewhere between Elsasser's and Yamamoto's values. After testing with many alternatives, the dashed curve in Fig. 2,

$$d\epsilon/dx = 0.17 - 0.0164 \cdot x - 0.0135 \cdot x^2, \quad x = \log u, \tag{11}$$

which obeys the above rules, was also found to give a good fit to the RW cooling rate. The emissivity curve now becomes

$$\epsilon = 0.60 + 0.17 \cdot x - 0.0082 \cdot x^2 - 0.0045 \cdot x^3, \quad x = \log u \tag{12}$$

where the constant 0.60 was found to give the best fit to RW in the integration method. (The Sasamori and cts schemes do not depend on this constant.) The suggested emissivity (12) is compared to some other emissivities in Table 2. It is close to Staley and Jurica's (1970) values.

The reason for Yamamoto's high values of $d\epsilon/dx$ for high x in Fig. 2 is probably that he did not allow

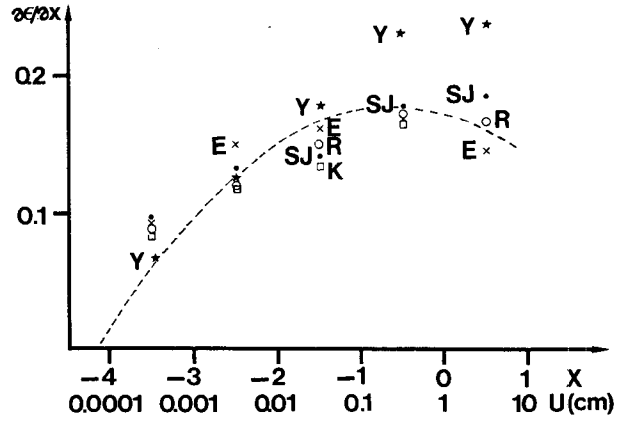

FIG. 2. $d\epsilon/dx$ calculated from given water vapor line spectrum emissivities. Y = Yamamoto (1952), E = Elsasser (1942), R = Robinson (1950), K = Kuhn (1963), SJ = Staley and Jurica (1970) CO_2-corrected. The dashed curve is Eq. (11). $x = {}_{10}\log(u)$, where u is the water vapor path length in cm.

TABLE 2. Water vapor emissivity estimates.

log$u$ cm^{-1}	−4	−3	−2	−1	0
Elsasser (1942)	.030	.117	.267	.437	.604
Robinson (1950)	.023	.105	.225	.375	.540
Yamamoto (1952)	.027	.093	.215	.393	.622
Kuhn (1963)	.040	.128	.249	.381	.543
Staley and Jurica (1970)	.076	.146	.277	.417	.590
Eq. (12)	.077	.138	.263	.426	.600

for spectral overlapping of H_2O with CO_2 (which was to be done separately on another chart). The Staley and Jurica values in Fig. 2 are, on the other hand, based on their overlap correction tables used with typical CO_2 pathlengths. If the same overlap correction is also applied to Yamamoto's ϵ, his $d\epsilon/dx$ values come close to the dashed curve in Fig. 2. The strong overlap also explains why $d\epsilon/dx$ tends down for high x.

With the new emissivity curve (12), the results of the three methods, shown in Fig. 3, become close to the RW cooling rate. They are further tested on three other cases, in which the RW cooling rates are available. These comparisons are in Fig. 4. Figure 4a is a moist tropical sounding (Fig. 11d of RW), Fig. 4b a typical midlatitude sounding (Fig. 7 of RW), and Fig. 4c a very cold and dry arctic sounding (Fig. 11e of RW) with a pronounced ground inversion. In these individual soundings the scatter in the heating rates is larger than in the monthly averaged data of Fig. 3. Also, the vertical resolution is high in the RW calculations whereas the tested fast methods use only the sounding data levels given in RW and thereby smooth the vertical heating profile. However, the cts method is again reasonably accurate.

b. Sensitivity tests

The integration, Sasamori, and cts methods are all very sensitive to the emissivity curve $\epsilon(u)$ chosen, as can be seen by comparing Figs. 1 and 3. Having now fixed ("optimized") the emissivity to Eq. (12), the other parameters may be varied.

In the Sasamori method (8), the ground temperature is clearly defined but the temperature at the "top" is more flexible. In a coarse vertical resolution, it could represent that part of the upper atmosphere which is not resolved, for instance, the mean temperature of the stratosphere. In Fig. 3 the Sasamori method cooling rate is calculated using three values of T_t: 0, 180, and 210 K. Clearly, the best result is obtained with T_t set to 0, in which case the Sasamori method comes close to the cts scheme. Sasamori's idea of a radiative water vapor source above the troposphere is therefore not supported by this comparison, perhaps because the amount of water vapor in the stratosphere is very small indeed. (In principle, T_t should be set to 3 K, instead of 0 K, to represent the "big bang" background radiation still present in the space. This tiny value does not make any difference to the present calculations however.)

The effect of varying the pressure scaling factor, n, in the cts method is in Table 3. Here, the midlatitude temperature and moisture profile (Fig. 4b) is used and n goes through 0 (no scaling), 0.5, 0.85 and 1.2 (more than linear scaling). The difference between the two extremes in n is about 0.4 K day^{-1} in the cooling rates, with $n = 0$ tending to give a flat rate with height and $n = 1.2$ a rate with much more cooling near the surface than higher up. In the range of $n = 0.5 \cdots 0.9$, suggested by Stephens (1984), the midlatitude cooling rate is not, however, very sensitive to n: the cooling rates vary only 0.12 K day^{-1} at most. Thus the exact value of n is not of great importance.

Having fixed $\epsilon(u)$ and n, the only variables in the cts scheme are the vertical resolution, and the temperature and moisture values. The effect of the vertical resolution has been tested in many articles (e.g., RW; Morcrette and Fouquart 1985) with the obvious result that finer resolution gives better results. We do not make any extra comparison here but just note that the smoother cooling rates in Fig. 4 may be partly due to the coarser vertical resolution in our calculations compared to RW.

Calculations with the three emissivity methods, where the temperature and moisture profiles were biased, gave results similar to those in RW: systematic increase/decrease of 1 K in T or T_d will give about 1.5% increase/decrease in the cooling rate. Random

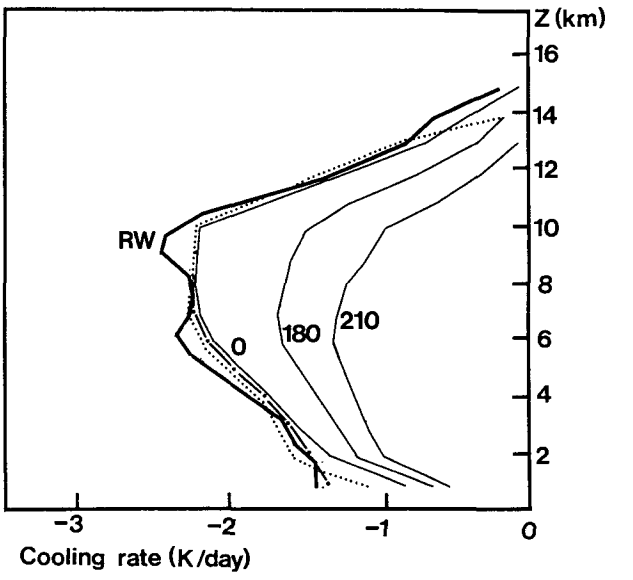

FIG. 3. Same as Fig. 1, but $\epsilon(u)$ is from Eq. (12). T_t in the Sasamori method is set to 0, 180, or 210 K as indicated.

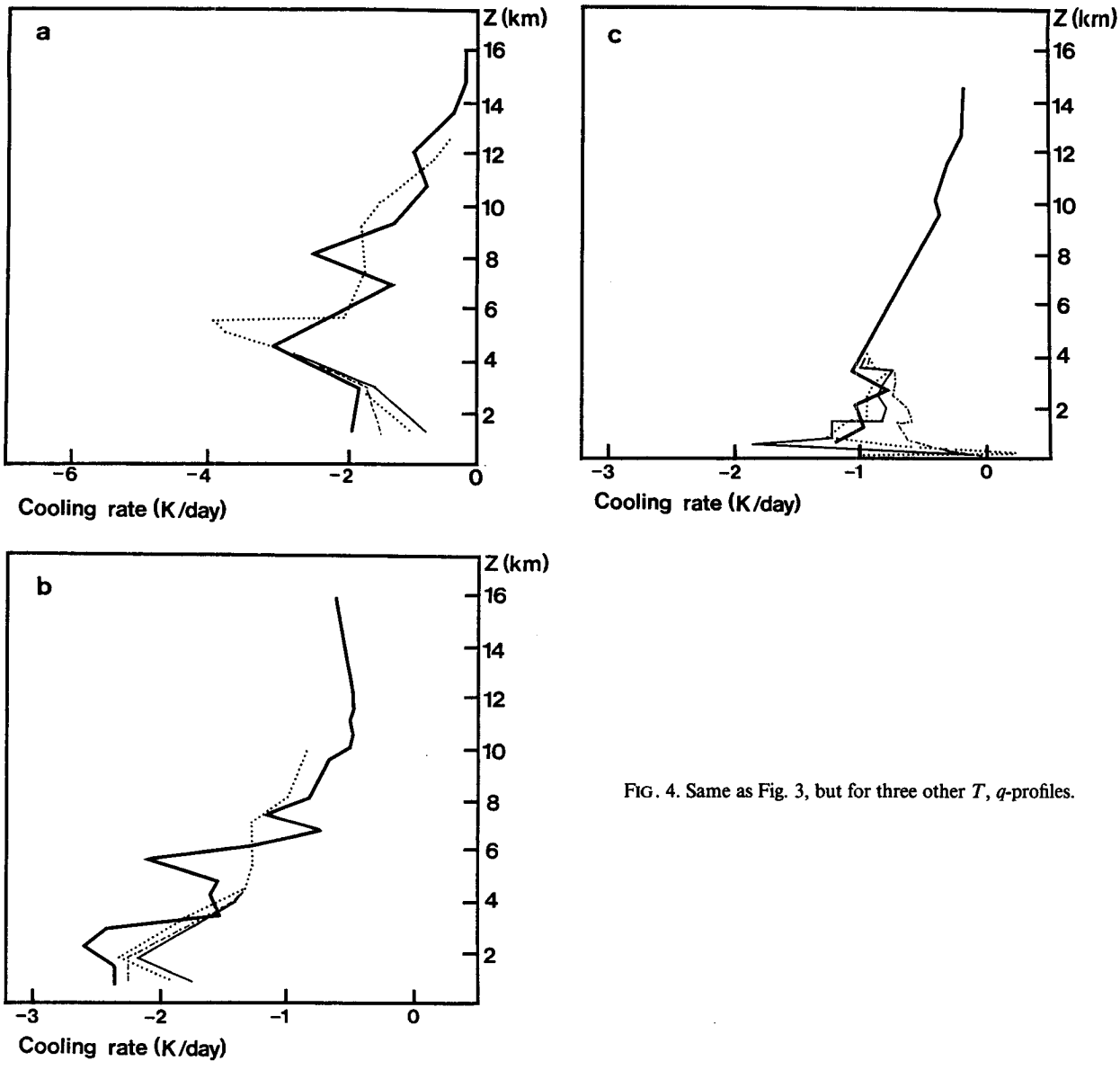

FIG. 4. Same as Fig. 3, but for three other T, q-profiles.

differences within 1 K in T or T_d along their profiles will give differences of about 5% in the cooling rates.

c. *Other effects on longwave cooling*

Based on, e.g., Liou (1980) and Paltridge and Platt (1976), the additional effect of CO_2, O_3 and other gases on the longwave radiative cooling rate seems to be quite small and vertically constant in the troposphere (of the order of 0.1 K day^{-1}), if any moisture is present. Also the cooling rate caused by aerosol absorption is small and not known very well; a few tenths of K day^{-1} has been suggested for Los Angeles, where even an "average" aerosol concentration is probably quite high (Ackerman et al. 1976). For a fast radiative cooling calculation in a short range model, one may thus simply add an extra constant cooling rate of $-0.1 \ldots 0.2$ K day^{-1} to represent their average effect, especially if cts or Sasamori methods are used for water vapor. (These methods are not very accurate for carbon dioxide radiation calculations.)

The water vapor continuum (the water vapor window) is now known to have more absorption/emission than the theoretical line spectra calculations indicate. Water vapor polymers [e.g., $(H_2O)_2$] or the far wings of nearby lines are both suggested as reasons for that. Whatever the reason, this less-than-perfect transparency in the window region seems to depend strongly

TABLE 3. Cooling rates in K day^{-1} (Fig. 4b) for different values of n.

p mb	$n = 0$	0.50	0.85	1.20
908	−2.00	−2.15	−2.26	−2.36
812	−1.97	−2.15	−2.27	−2.38
724	−1.62	−1.79	−1.90	−2.00
645	−1.33	−1.47	−1.56	−1.65
572	−1.08	−1.18	−1.25	−1.31
506	−1.10	−1.18	−1.23	−1.27
446	−1.22	−1.27	−1.30	−1.31
393	−1.27	−1.29	−1.28	−1.26
344	−1.08	−1.06	−1.02	−0.96
301	−1.17	−1.06	−0.95	−0.82
262	−1.40	−1.11	−0.89	−0.67

on water vapor pressure. Thus, strong cooling is expected near the surface in the tropics.

In Fig. 5 the cooling rate based on the mean of 14 clear air radiometer soundings on two tropical islands is shown (Cox 1969). It is rather close to the RW profile in Fig. 1, except near the ground. The dashed line gives the cts approximation using Cox' data. The dotted line is the cts approximation plus a constant −0.1 K day^{-1} (parameterizing the effect of other gases and aerosol) plus $-0.001q^3(z)$ (q in g kg^{-1}), which parameterizes as a simple (least squares) approximation on the strong dependency of the continuum effect on water vapor pressure. This last effect is only important in the moist tropics and may be left out elsewhere.

The cts scheme and the other suggested simple parameterizations seem to give a fairly good fit to the observed longwave cooling rate in the tropical case. Unfortunately, little data is available for higher latitude comparisons. The tethered balloon observations of Moores (1982) in south England give a cooling rate of −1 . . . −2 K day^{-1} for the 150–1000 m layer during clear summer days, which is in accordance with the suggested parameterizations.

d. Downcoming radiation at the surface

In a forecast model, the downcoming longwave radiation at the surface is an important factor in the surface heat budget. It should, therefore, be given correctly by the radiation scheme. Equation (3) can be used to produce $F^{\downarrow}(sfc)$. If ϵ from Eq. (12) is used in (3), the downcoming flux is at all tropospheric heights within 5 W m^{-2} with those reported in RW. It thus seems that (3) and (12) provide a fast and relatively accurate way of producing the downcoming radiation from the water vapor line spectrum at the surface.

These values are, however, much smaller than those observed. (In fact, the low values were the main reason for Sasamori to introduce the Yamamoto $\epsilon(u)$, which produces large surface fluxes but also too much cooling.) The reason for the low values is probably that continuum, other gases, and aerosols give a sizable downradiation, especially near the surface. In a recent comparison of many radiation schemes (Luther et al. 1988), the average $F^{\downarrow}(sfc)$ of several line-by-line schemes in a midlatitude summer atmosphere case was 267 W m^{-2}, if water vapor line spectrum only was considered. When the continuum effect was added, $F^{\downarrow}(sfc)$ increased to 326 W m^{-2}, and with CO_2, O_3 it increased further to 342 W m^{-2}. These and other values in the comparison suggest that a very simple parameterization of $F^{\downarrow}(sfc)$ (in W m^{-2}) could be

$$F^{\downarrow}(sfc) = F^{\downarrow}_{wl}(sfc) + 4 \cdot q(sfc) + 16 \qquad (q \text{ in g kg}^{-1}). \quad (13)$$

Here, $F^{\downarrow}_{wl}(sfc)$ is calculated using (3) and (12), $4 \cdot q(sfc)$ gives the continuum addition, and 16 W m^{-2} is a constant addition from CO_2, O_3 and aerosols in a moist atmosphere. This simple parameterization also produces sensitivity for a change in the water vapor mixing ratio (1.25× vs. 0.75× normal values), which is similar to those of the line-by-line models ($\Delta F^{\downarrow}(sfc) = 45$ W m^{-2}) reported in Luther et al. (1988).

e. Clouds

In the interest of fast calculations, all clouds are assumed dense or thick enough to be black in the thermal

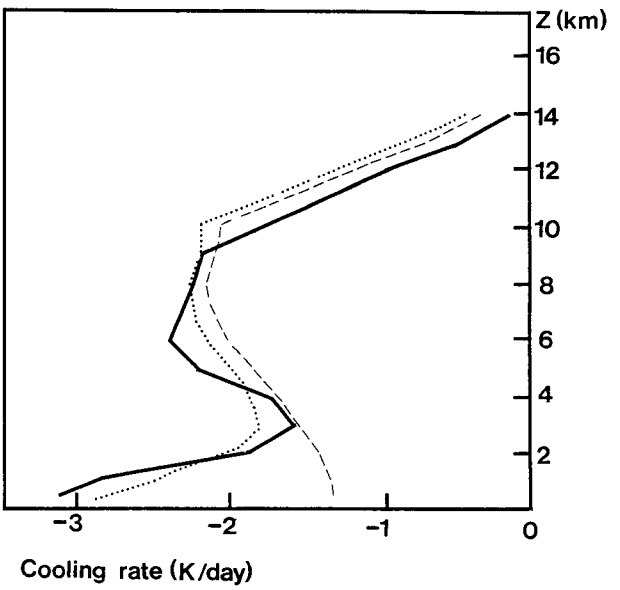

FIG. 5. The cooling rate from Cox' (1969) radiometer observations (thick line), the cts approximation for water vapor line spectrum absorption (dashed line), and the cts approximation plus the suggested simple parameterizations for other effects (dotted line).

infrared. Although this is not strictly true, the coarse vertical resolution of the targeted atmospheric host models (a few hundred meters in the upper boundary layer and much more higher up) guarantees that even cirrus clouds will be thick enough to appear nearly black.

Below and between cloud layers one thus assumes that the ground or the cloud deck below and the cloud base above are black surfaces at their respective temperatures. The Sasamori scheme (8) is then used in these layers. Above the highest cloud layer one may use the cts scheme (10). For the downcoming radiation at the surface one may simply set it equal to the black radiation at the lowest, cloud base temperature, perhaps slightly enhanced on the way down through use of (3).

What about inside the clouds? Although several investigations suggest that the (infrared) radiative cooling near the cloud top is very strong in a shallow layer, and somewhat weaker heating prevails near the cloud base, our recommendation here is simple: do nothing, i.e. set the radiative temperature change to zero inside clouds. The reason is that if one sets up a complex radiation scheme inside the clouds, one should also consider all the other effects important for cloud dynamics (e.g., entrainment, droplet accumulation, and evaporation). Since these are not simulated in the intended host models, it is perhaps best to exclude also the relatively strong radiation drive in the cloud layers also.

If, however, a fast radiation scheme inside the clouds is considered necessary (and the vertical resolution of the host model is sufficient), the recent scheme of Hanson and Derr (1987) is recommended.

4. Shortwave parameterization

Solar radiation is important in short-range high-resolution modeling mainly because of daytime surface heating of land, especially in clear conditions. Therefore, the strategy here is to adjust the solar flux at the surface (to be used in the host model's land surface temperature budget) close to observations.

The solar constant (in W m^{-2}) is given by

$$S = 1365 \cdot (1 + 0.03422 \cos(d \cdot 2\pi/365) + 0.00128 \cdot \sin(d \cdot 2\pi/365)) \quad (14)$$

where d is the running date from 1 January. Here, the annual distance change of the earth from the sun has been taken into account to within 1 W m^{-2} (Pielke 1984.) At latitude f and local solar hour t, the sine of the local sun height angle h (cosine of the zenith angle) is given by

$$\sin(h) = \cos(f)\cos(dc)\cos((t - 12) \cdot 2\pi/24) + \sin(f)\sin(dc) \quad (15)$$

where $dc = 23.45° \cdot \cos[(d - 172) \cdot 2\pi/365]$ is the declination angle. Here, $S \cdot \sin(h)$ now gives the solar radiation falling on a horizontal plane in any (modeled or real) local time and latitude, if there were neither absorption nor scattering in the atmosphere. These gaseous and aerosol attenuation effects should now be added in a simple fashion.

a. *Surface global solar flux in clear air*

The global (direct + diffuse) downward solar radiation at the surface is obtained by reducing $S \cdot \sin(h)$ through the parameterized broadband depletions by:

i) ozone ultraviolet and visible absorption, mainly in the stratosphere. Here, using 0.35 cm (the global average) of O_3 at NTP, a simple curve $0.024 \cdot (\sin h)^{-0.5}$ gives a good fit to Lacis and Hansen's (1974, hereafter LH) more elaborate scheme. If more accuracy is needed, the amount x of ozone (in cm) may be given for each month and latitude with 0.024 replaced by $0.024 + (x - 0.35) \cdot 0.03$.

ii) H_2O and the smaller CO_2, O_2 overlapping infrared absorptions in the troposphere. A simple curve $0.11 \cdot (u/\sin h)^{0.25}$ gives a reasonable fit to Yamamoto's (1962) results (curve 6 in his Fig. 1) for the typical values of $u/\sin h \sim 0.1 \ldots 10$ cm where $u = u(0, \infty)$ is the pressure-scaled water vapor amount from (7).

iii) Rayleigh scattering from air molecules. The LH scheme was adopted, where the broadband albedo of pure Rayleigh scattering for direct solar beams is $0.28/(1 + 6.43 \cdot \sin h)$, and for the reflected beams, 0.0685. Comparison of these with Coulson's (1959) calculations shows that the LH parameterization is fairly good. Neglecting the (very small) multiple reflection effect, the backscattering from the reflected beams is simply $0.07 \cdot \alpha$, where α is the albedo of the surface in the visible part of the solar spectrum ($\sim$0.05 over sea, 0.2 over land, 0.7 over snow and ice).

With coefficients "aa" and "as" (≥ 1) for a crude inclusion of aerosol absorption and scattering as enhancing the gaseous and molecular effects listed above, the global surface flux is now given as

$$s^{\downarrow}(sfc) = S \sin h \{1 - 0.024(\sin h)^{-0.5} - \mathrm{aa} \cdot 0.11(u/\sin h)^{0.25} - \mathrm{as} \cdot (0.28/(1 + 6.43 \cdot \sin h) - 0.07\alpha)\}. \quad (16)$$

This parameterization was tested in the 5-year observations of global solar radiation at Aspendale (Australia) during clear days (Fig. 6.3 in Paltridge and Platt 1976). The annual mean atmospheric water content of 1.5 cm at Aspendale (reduced by 15% because of

the pressure scaling) was used as u, and surface albedo of 20% was assumed. With aa and as = 1 (i.e. no aerosols) the parameterization (16) produced the upper envelope of the Aspendale observations (i.e. those made in clean air). It was 5% (20–40 W m^{-2}) too large when compared with the mean of all observations. The difference presumably is caused by the average aerosol extinction. The difference was reduced to less than 2 W m^{-2} at all $h > 10°$ by setting aa = 1 and as = 1.9; i.e. assuming no aerosol absorption but extra scattering 90% above the pure molecular scatter level. That the aerosol absorption is quite small in the Australian east coast during normal visibility was demonstrated in the flight observations of Paltridge (1973). The values aa = 1, as = 1.9 are thus tentatively suggested for coastal, ocean, and other areas with mostly small and transparent background aerosol particles (sea salt), which scatter but do not absorb sunlight.

The parameterization (14)–(16) was further tested against Tammelin et al. (1987), who have made careful observations of the global solar radiation at Pernaja (South Finland) during clear and cloudy days; $u(0, \infty)$ was calculated from the nearest radio sounding at Jokioinen, Finland. Also in these data, use of aa = as = 1 gave a 5% overestimate during all seasons and hours. Here, the selection of aa = 1.2, as = 1.25 gave the best fit to the observations (error < 5 W m^{-2}), suggesting that in the continental air over north Europe the aerosol scattering adds 25% to the Rayleigh scatter, and the aerosol particles include enough black material to increase absorption 20% over the gaseous absorption. From the 5% total extra depletion, aerosol absorption explains about 3%, and scattering, 2%. These values are compatible with the surface and flight estimates of Robinson (1966) and Roach (1961) over Britain. It may be noted that also in those Paltridge's flight observations, which were made during hazy days with low visibility due to dust storms and bush fires, extra absorption was found with a suggested value of aa $\approx$ 1.3–1.5.

The choice of aa = 1.2 and as = 1.25 is thus suggested for use in (16) over continental industrialized areas during normal visibility. Since the aerosol absorption and scattering is in itself an extremely complex matter, this crude simulation can be defended only on the basis of simplicity and speed.

b. *Solar heating in clear air*

Since scattering just redistributes the solar beam energy, only absorption a enters to the net flux divergence. Thus the solar heating becomes

$$\left(\frac{\partial T}{\partial t}\right)_{\text{SWR}} = \frac{1}{\rho c_p}\frac{\partial}{\partial z}(s^{\downarrow} - s^{\uparrow}) = -\frac{g}{c_p} S \sin h \frac{\partial a}{\partial p}. \quad (17)$$

In the troposphere, water vapor is the strongest gaseous absorber. Chou (1986) developed a fast and fairly accurate broadband parameterization for it, based on comparisons with line-by-line calculations. Chou also showed that the LH scheme [based on Yamamoto's (1962) absorption data] is not bad, its error being ~0.2 K day^{-1}. These two schemes can be recommended. Both calculate the heating (17) by finite differencing $\partial a/\partial p$. Here we suggest an alternative, which is even faster and is potentially more accurate, since $\partial a/\partial p$ is obtained analytically.

Using linear pressure scaling, $\partial u = q\cdot(p/p_o)\partial p/g$ so that $g\cdot\partial a/\partial p = q\cdot(p/p_o)\cdot\partial a/\partial u$. From Chou's (1986) line-by-line results (his Fig. 6), the curve $\partial a/\partial u$ can be approximated with good accuracy by the simple functions

$$\partial a(u)/\partial u = y(u) = \begin{cases} 0.029u^{-0.81} & u \geqq 0.05 \text{ cm} \\ 0.050u^{-0.63} & u < 0.05 \text{ cm} \end{cases} \quad (18)$$

where u is the linearly pressure-scaled vertical water vapor amount (in cm; (7) with $n = 0.85$ can also be used without much error). For the range $0.2 < u < 3$ cm (18) is also close to Yamamoto's (1962) absorption values (and thus the LH scheme), which in Paltridge's (1973) flight data described the attenuation of the net flux rather well. For slant direct paths $u = u/\sin h$ and $y(u)$ is replaced by $y(u/\sin h)/\sin h$. The isotropically reflected beams experience path lengths of $u_* = u(0, \infty)/\sin h + u(0, z)\cdot 1.67$, and (18) becomes $\alpha\cdot 1.67\cdot y(u_*)$ for them. This parameterization [(17)–(18)] gives results within 0.1 K day^{-1} with Chou's scheme, which itself was within 0.1 K day^{-1} with the line-by-line calculations for water vapor.

Calculations for the smaller CO_2, O_2, and O_3 absorptions using the standard absorption curves of Sasamori et al. (1972) resulted in a total effect that is fairly constant in height and is given by $0.15\cdot(\sin h)^{0.3}(\pm 0.02)$ K day^{-1}, below 300 mb. Thus the suggested solar heating over oceans and other areas with negligible aerosol absorption becomes (in K s^{-1})

$$\left(\frac{\partial T}{\partial t}\right)_{\text{SWR}} = S\left(\frac{q}{c_p}\right)\left(\frac{p}{p_o}\right)\{y(u(z, \infty)/\sin h) + \alpha\cdot 1.67 \times y(u_*)\sin h\} + 1.7\cdot 10^{-6}(\sin h)^{0.3}. \quad (19)$$

Here, y is given by (18) and α is the surface albedo. The $y(u_*)$ term (water vapor absorption in the reflected beam) is non-negligible only in the boundary layer.

In continental air, especially over industrialized areas, the coefficient 0.029 in (18) may tentatively be increased to 0.04–0.05 near the surface to account crudely for the extra aerosol absorption reported for example in Paltridge (1973) and Roach (1961).

c. Clouds

In cloudy days, Atwater and Ball (1981) suggest a constant cloud transmission function, t_C, for each cloud type; e.g., 0.15 for stratus and nimbostratus, 0.40 for altostratus, and 0.9 for cirrus. Also the observations of Tammelin et al. (1987), made during overcast days with stratus-type cloud, support the view that (16) multiplied by $t_C = 0.3$ gives a reasonable first-guess for the surface total solar flux during overcast days. If the host model is intelligent enough to separate between different cloud types, Atwater and Ball's (1981) t_C constants, the LH scheme, or Hanson and Derr's (1987) scheme can be used. However, in the present-day limited-area short-range forecast and mesoscale models, "cloud" is typically defined by relative humidity exceeding a threshold value without any detailed knowledge of the water amount or optical thickness in the cloudy layers. Then, multiplying (16) and (19) by 0.3, is a fast first parameterization producing reasonable solar surface fluxes and heating below clouds, which is close to that from LH's more complex scheme, except perhaps for cirrus clouds.

In short, the parameterization suggested above is a simplification of the LH scheme with additions of CO_2, O_2, and average aerosol effects. The parameterization reproduces the surface flux with good accuracy and is not far from line-by-line model results in the solar heating calculation for gaseous absorption. Yet it is very fast and includes the most important feedback mechanisms. Clouds are handled in a very simple way but with acceptable accuracy for a short-range model.

5. Summary

Three longwave emissivity parameterization schemes were tested against a reference narrowband model in clear conditions (no clouds). The crucial factor proved to be the emissivity dependence on the water vapor path length; a candidate is given as Eq. 12. The three schemes (direct integration, Sasamori, and cooling-to-space) gave almost identical results in the present cases. The sensitivity of the Sasamori and cts schemes to variations in their parameters was tested.

For the other gases and aerosols in the troposphere a constant cooling rate of $-0.1 \ldots 0.2$ K day^{-1} was suggested, and for the water vapor continuum effect, a simple q^3 dependence seems to be adequate. The longwave downward radiation at the surface was discussed and methods were presented as well as the cloudy case.

For the shortwave part, Lacis and Hansen's (1974) and Chou's (1986) methods were simplified and augmented with average aerosol effects. The use of these gave a satisfactory fit to surface and flight observations.

The suggested methods should give an extremely fast radiation parameterization package, to be used for example in short-range high-resolution or mesoscale-atmospheric models, or in land-surface heat budget calculations. The inputs needed are the temperature and moisture profiles (e.g., in a grid point of a model, or as observed in a radio sounding). The outputs are the net radiative heating at all data levels and the downcoming longwave and shortwave fluxes at the surface. The accuracy of the clear-sky shortwave results (0.2 K day^{-1} for heating, 10 W m^{-2} for fluxes) approaches the accuracy of the available measurements. The longwave part is less accurate but could be improved with better observations or when line-by-line model results become available.

REFERENCES

Ackerman, T. P., K. N. Liou and C. B. Leovy, 1976: Infrared radiative transfer in polluted atmospheres. *J. Appl. Meteor.*, **15,** 28–35.

Atwater, M. A., and J. T. Ball, 1981: A surface solar radiation model for cloudy atmospheres. *Mon. Wea. Rev.*, **109,** 878–888.

Chou, M.-D., 1986: Atmospheric solar heating in the water vapor bands. *J. Appl. Meteor.*, **25,** 1532–1542.

Coulson, K. L., 1959: Characteristics of the radiation emerging from the top of a Rayleigh atmosphere. *Planet. Space Sci.*, **1,** 256–284.

Cox, S. K., 1969: Observational evidence of anomalous infrared cooling in a clear, tropical atmosphere. *J. Atmos. Sci.*, **26,** 1347–1349.

Elsasser, W. M., 1942: Heat transfer by infrared radiation in the atmosphere. *Harvard Meteor. Studies,* **6,** Harvard University, 107 pp.

Fels, S. B., and M. D. Schwartzkopf, 1975: The simplified exchange approximation: A new method for radiative transfer calculations. *J. Atmos. Sci.*, **32,** 1475–1488.

Garand, L., 1983: Some improvements and complements to the infrared-emissivity algorithm including a parameterization of the absorption in the continuum region. *J. Atmos. Sci.*, **40,** 230–244.

Goody, R. M., 1964: *Atmospheric Radiation.* Oxford University, 436 pp.

Hanson, H. P., and V. E. Derr, 1987: Parameterization of radiative flux profiles within layer clouds. *J. Clim. Appl. Meteor.*, **26,** 1511–1521.

Houghton, H. G., 1984: *Physical Meteorology.* Massachusetts Institute of Technology, 422 pp.

Kondratyev, J., 1969: *Radiation in the Atmosphere.* Academic, 912 pp.

Kuhn, J. V., 1963: Radiometersonde observations and infrared flux emissivity of water vapor. *J. Appl. Meteor.*, **2,** 368–378.

Lacis, A. A., and J. E. Hansen, 1974: A parameterization for the absorption of solar radiation in the earth's atmosphere. *J. Atmos. Sci.*, **31,** 118–133.

Liou, K. N., 1980: *An Introduction to Atmospheric Radiation.* Academic, 392 pp.

Luther, F. M., R. G. Ellingson, Y. Fouquart, S. Fels, N. A. Scott and W. J. Wiscombe, 1988: Intercomparison of radiation codes in climate models: Longwave clear-sky results—a workshop summary. *Bull. Amer. Meteor. Soc.*, **69,** 40–48.

McNider, R. T., and R. A. Pielke, 1981: Diurnal boundary-layer development over sloping terrain. *J. Atmos. Sci.*, **38,** 2198–2212.

Morcrette, J.-J., and Y. Fouquart, 1985: On systematic errors in parameterized calculations of longwave radiation transfer. *Quart. J. Roy. Meteor. Soc.*, **111,** 691–708.

Paltridge, G. W., 1973: Direct measurements of water vapor absorption of solar radiation in the free atmosphere. *J. Atmos. Sci.*, **30,** 156–160.

——, and C. M. R. Platt, 1976: *Radiative Processes in Meteorology and Climatology.* Elsevier, 318 pp.

Pielke, R. A., 1984: *Mesoscale Meteorological Modeling.* Academic, 612 pp.

Roach, W. T., 1961: Some aircraft observations of fluxes of solar radiation in the atmosphere. *Quart. J. Roy. Meteor. Soc.*, **87,** 346–363.

Robinson, G. D., 1950: Notes on the measurement and estimation of atmospheric radiation. *Quart. J. Roy. Meteor. Soc.*, **76,** 37–51.

——, 1966: Some determinations of atmospheric absorption by measurement of solar radiation. *Ibid.*, **92,** 263–269.

Rodgers, C. D., 1967: The use of emissivity in atmospheric radiation calculations. *Quart. J. Roy. Meteor. Soc.*, **93,** 43–54.

——, 1977: Radiative processes in the atmosphere. ECMWF Seminars, Reading, 5–66.

——, and C. D. Walshaw, 1966: The computation of infrared cooling rate in planetary atmospheres. *Quart. J. Roy. Meteor. Soc.*, **92,** 67–92.

Sasamori, T., 1968: Radiative cooling calculation for application to general circulation experiments. *J. Appl. Meteor.*, **7,** 721–729.

——, 1972: A linear harmonic analysis of atmospheric motion with radiative dissipation. *J. Meteor. Soc. Japan,* **50,** 505–517.

——, J. London and D. Hoyt, 1972: Radiative budget of the Southern Hemisphere. *Meteor. Monogr.*, **35,** 9–23.

Staley, D. O., and G. M. Jurica, 1970: Flux emissivity tables for water vapor, carbon dioxide and ozone. *J. Appl. Meteor.*, **9,** 365–372.

Stephens, G. L., 1984: Review of the parameterization of radiation for numerical weather prediction and climate models. *Mon. Wea. Rev.*, **112,** 826–867.

Tammelin, B., M. Pietarinen and A. Peltomaa, 1987: On the global radiation incident variously orientated surfaces on the south coast of Finland. Meteorological Publ., **5,** Finnish Meteor. Institute.

Washington, W. M., and D. L. Williamson, 1977: A description of the NCAR global circulation models. *Methods in Computational Physics,* **17,** Academic.

Wu, M.-L., 1980: The exchange of infrared radiative energy in the troposphere. *J. Geophys. Res.*, **85,** 4084–4090.

Yamamoto, G., 1952: On a radiation chart. Scientific rep., Tohoku University, Ser. 5.

——, 1962: Direct absorption of solar radiation by atmospheric water vapor, carbon dioxide and molecular oxygen. *J. Atmos. Sci.*, **19,** 182–188.